

# Segmentation of liver region with tumorous tissues

Xuejun Zhang<sup>\*a,c</sup>, Gobert Lee<sup>a</sup>, Tetsuji Tajima<sup>a</sup>, Teruhiko Kitagawa<sup>a</sup>, Masayuki Kanematsu<sup>b</sup>,  
Xiangrong Zhou<sup>a</sup>, Takeshi Hara<sup>a</sup>, Hiroshi Fujita<sup>a</sup>, Ryujiro Yokoyama<sup>b</sup>, Hiroshi Kondo<sup>b</sup>, Hiroaki  
Hoshi<sup>b</sup>, Shigeru Nawano<sup>d</sup> and Kenji Shinozaki<sup>e</sup>

<sup>a</sup> Department of Intelligent Image Information, Division of Regeneration and Advanced Medical  
Sciences, Graduate School of Medicine, Gifu University, Gifu 501-1194, Japan

<sup>b</sup> Department of Radiology, Gifu University School of Medicine and University Hospital,  
Gifu 501-1194, Japan

<sup>c</sup> College of Computer Science and Information Engineering, Guangxi University,  
Nanning, Guangxi 530004, P. R. China

<sup>d</sup> Department of Radiology, National Cancer Center Hospital East, Chiba 277-8577, Japan

<sup>e</sup> National Kyushu Cancer Center, Kyushu, Fukuoka 811-1395, Japan

## ABSTRACT

Segmentation of an abnormal liver region based on CT or MR images is a crucial step in surgical planning. However, precisely carrying out this step remains a challenge due to either connectivities of the liver to other organs or the shape, internal texture, and homogeneity of liver that maybe extensively affected in case of liver diseases. Here, we propose a non-density based method for extracting the liver region containing tumor tissues by edge detection processing. False extracted regions are eliminated by a shape analysis method and thresholding processing. If the multi-phased images are available then the overall outcome of segmentation can be improved by subtracting two phase images, and the connectivities can be further eliminated by referring to the intensity on another phase image. Within an edge liver map, tumor candidates are identified by their different gray values relative to the liver. After elimination of the small and non-spherical over-extracted regions, the final liver region integrates the tumor region with the liver tissue. In our experiment, 40 cases of MDCT images were used and the result showed that our fully automatic method for the segmentation of liver region is effective and robust despite the presence of hepatic tumors within the liver.

**Keywords:** Segmentation, Liver, Tumor, Multi-phase CT, Edge extraction, Subtraction method, Computer-aided diagnosis

## 1. INTRODUCTION

The liver is the largest organ in the body, and it involves almost all the biochemical pathways that function in allowing growth, fighting disease, supplying nutrients, providing energy, and aiding reproduction. Of the total blood pumped out with each heartbeat, 25% reaches the liver; in fact, the liver receives blood from two blood vessels—the portal vein and the hepatic artery. This additional blood supply facilitates the spread of metastatic tumors present in other organs into the liver. Cancer may develop directly in the liver (primary) or spread from other sites (metastatic or secondary) via the circulatory or lymphatic systems. Primary malignant liver tumor includes hepatocellular carcinoma (HCC), cholangiocellular carcinoma (CCC) and both (mixed tumor); HCC and CCC are considered the most important types of carcinomas in clinical practice, and 90% of the cancers are cases of HCC that cause 1.25 million deaths per year worldwide [1]. Currently, surgery, either by resection (removal of the tumor) or liver transplantation, offers the only chance to cure liver cancers such as HCC and some other types of metastatic liver cancers including those that metastasize from the colon and rectum.

Multidetector CT (MDCT) is currently used as the diagnostic modality of choice for the detection, characterization, and determination of the precise location of liver tumors. The recent introduction of MDCT has greatly enhanced image resolution and markedly decreased the time required for scanning, thereby enabling the examination of the whole

---

\*zhang@fjt.info.gifu-u.ac.jp; phone 81 58 230-6513; fax 81 58 230-6514

body within a few minutes; moreover, motion artifacts can be minimized because of its shorter acquisition time. Multiple image sets can then be obtained following infusion of a contrast agent, and focal liver diseases can be accurately detected on contrast material-enhanced CT scans. Prior to surgical treatment of liver tumors, computer-aided liver surgery has proven to be a useful tool for supporting radiologists and surgeons in planning liver resections or living donor transplantation by using multi-phase MDCT images. Some research groups developed tools such as software to facilitate image interpretation or commercial kits and interactive equipment for surgeons to be used in preoperative planning. However, numerous limitations of these tools, including excessive time requirement and involvement of several manual steps or complicated procedures limited their clinical use. Development of a fast and fully automatic algorithm may help solve the abovementioned problems.

We have been developing a computer-aided diagnosis (CAD) system for the detection and characterization of the pathologies of focal liver lesions on MR images [2], as well as an automatic method for the segmentation of liver region on MRI [3]. Our previous method is based on the edge detection algorithm with the main focus on MR images. Although our method is effective in the segmentation of cirrhotic liver images, some liver regions are not successfully extracted due to the presence of hepatic lesions within the liver. In this paper, we propose a fully automatic method to segment the liver and other organs on multi-phase CT images despite the presence of hemangioma or tumors such as HCC within the liver. Such a “Press-One-Button” system is extremely user-friendly and can be used without any training; moreover, it provides highly accurate 3D images of different organs. This system can be an effective first step in developing methods to reduce the manual processing time.

The challenge of a liver segmentation technique is to robustly extract the liver regions with lesions or regions that have received partial transplants. The liver not only has radiodensity that is similar to its surrounding structures resulting in the common problem of connectivities to the heart, stomach, or kidney but it is also affected by hepatic diseases that may change its shape and internal texture or homogeneity. In addition, the image quality from different modalities varies in terms of signal-to-noise ratio, motion artifacts, etc. There are some reports on the segmentation of the abdominal organs on CT images by using a thresholding method, likelihood function, or hepatic vessels [4–6]. However, many reports address only techniques involving segmentation of the normal liver tissues and these techniques cannot usually be used for extracting the abnormal liver regions. Bae et al. [7] used a thresholding method to segment the liver in living-donor abdominal CT images. In this method, a gray-level threshold was determined from the histogram; therefore, the segmentation would be affected by the presence of large hepatic tumors with different intensity within the liver or other connected organs and by the tissues that had overlapping density. Park et al. [8] presented their method to construct a probabilistic atlas of an abdomen comprising four organs. By registering each organ separately, better overall accuracy was obtained even with non-contrast CT scans. However, manually putting 17 control points and selecting a reference patient renders the method impractical in clinical studies; moreover, it is difficult to construct some liver diseases on an “abnormal atlas.” For example, the morphological change in cirrhosis is extensive, and a partially transplanted liver does not have a regular shape. Therefore, constructing such an atlas is difficult. In order to ensure that our software known as LiverCAD can be widely used in different hospitals for different modalities, we used edge detection or combined with a subtraction processing algorithm that was not dependant on the intensity or noise of the CT images or on the accuracy of the MR images. To the best of our knowledge, there have been no other reports on such a method thus far.

## 2. MATERIALS AND METHODS

A brief illustration of abnormal liver segmentation is shown in Figure 1. Our method consists of three main steps: (1) Preprocessing the multi-phase images by smoothing and registration, (2) Detection the edges on one-phase image or two-phase-subtraction image to obtain an initial liver mask from which the tumors of different intensity are separated, (3) Eliminating the connectivity by comparing shape or different attenuation values from other phase images.

Three datasets from different hospitals were examined with different multi-detector row CT scanners. In the main dataset, an MDCT scanner (Aquilion; TOSHIBA, Japan) was used to scan a quadruple-phase protocol that included unenhanced, hepatic arterial, portal venous, and delayed phase images. Each patient received the contrast/bolus agent (Oypalomin370 or Optiray320) via a power injector at a rate of 3 ml/s, and the final average volume of contrast material was 100 ml (range, 110–182 ml). Four complete acquisitions of the entire liver were obtained in a craniocaudal direction during one breath hold with the following parameters: slice interval, 0.625–1.25 mm; bits stored, 16 bits; pixel-spacing, 0.50–0.625 mm; spatial resolution,  $512 \times 512$ ; 165 mAs; and 120 kVp. In all patients, non-contrast scanning (i.e., the

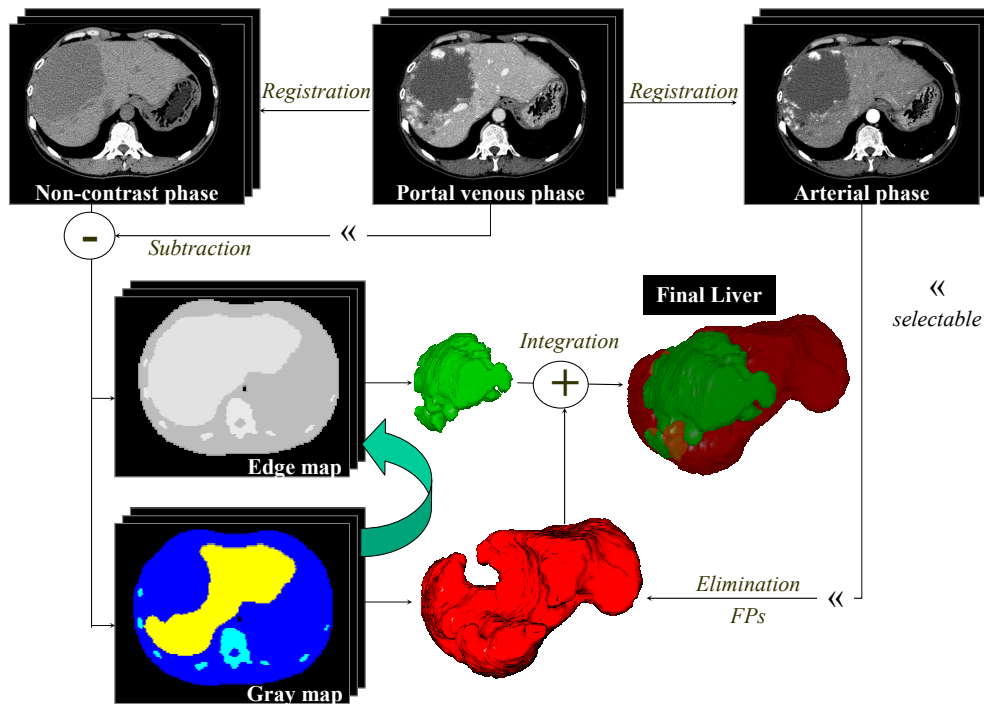


Fig. 1. An overall procedure of the segmentation of an abnormal liver region from MDCT based on edge detection and subtraction method.

first pass) was performed. The final average start time for the hepatic arterial phase was 37 s (range, 35–40 s). The portal venous phase and the equilibrium phase (i.e., the third and fourth passes, respectively) scans were acquired at 65 s (range, 60–70 s) and 180 s, respectively, after contrast material injection. These cases were categorized by experienced radiologists, and 12 normal cases, 32 cases with 44 HCC tumors, and 9 other tumor cases were confirmed.

## 2.1 Contrast-enhanced liver region with tumor tissues in abdominal CT images

Multi-phase contrast-enhanced CT is a recently developed improved liver imaging technique. In this technique, a complete set of images is obtained during the hepatic-arterial dominant phase of liver perfusion, followed by a second set that is obtained during the portal-venous phase, and the equilibrium phase images are taken at 3 min after the contrast agent is injected. In addition, unenhanced images are often used in clinical studies to provide supplementary information. Liver parenchyma as well as the hepatic veins and portal veins is well enhanced on the portal venous phase. Therefore, this phase is widely used for the liver and vessel segmentation prior to surgery. Some lesions such as HCC and certain metastatic tumors have higher attenuation values than the liver parenchyma during the arterial phase due to the blood supplied by the hepatic artery. Most metastatic tumors have a portal-venous blood supply and are hypoattenuating compared to the rest of the liver during the portal phase of perfusion. Hepatic hemangioma is a common benign liver tumor, which shows hypoattenuation similar to that of vessels on unenhanced CT. The hemangioma illustrated in Fig. 1 shows the contrast-enhanced CT scan obtained during arterial and portal venous phase with a large hypoattenuating mass having enhancing dots. Since the tumor pattern in the liver varies greatly in different cases, accurate segmentation of the liver region by computer requires the use of a more sophisticated algorithm than that only used for the normal liver. This factor has to be considered while developing a system for surgical planning since every patient has a different tumor pattern. Furthermore, other factors such as blurring artifacts or bad signal-to-noise ratio also increase the difficulties in segmentation.

## 2.2 Preprocessing for normalizing images

The preprocessing step is carried out to unify the different phase images under a standard condition, in which the position and size of the liver area or tumors are relatively the same, as well as to decrease the noises of images. The image datasets are first resampled to  $256 \times 256$  resolution to decrease the overall processing time, and then a  $3 \times 3$  median filter is applied to reduce the effect of the noise while enlarging the width of liver edge. Finally, registration of the portal venous phase 3D image to other phases is undertaken to ensure that the livers have identical shapes. Even though the images obtained are of the same patient, he/she may shift or change the breathing pattern during the 4 min of CT scanning. If more than one-phase image is required in the program, the registration step is crucial, especially, to extract a small HCC tumor, based on subtraction method. We compare three registration methods in this study:

### (a) *Affine based transformation:*

One coronal slice is selected on both two phase 3D images to be registered as fixed image  $I1(x,z)$  and moving image  $I2(x,z)$ . After a non-strict binarization processing, an error image  $E11-I2(x,z)$  can be calculated by the difference of the images of  $I1(x,z)$  and  $I2(x,z)$ . These procedures are repeated by changing the position of moving image  $I2(x,z+\delta Z)$  in a searching range. The optimized parameter  $\delta Z$  can be determined with the smallest numbers of pixels in  $E11-I2(x,z)$ .

### (b) *Thin-plate splines (TPS) based deformation:*

Eleven landmarks are selected manually on one phase CT images, and the corresponding points in the other phase images. These are one point at the centroid of the liver region that first appeared on the top slice near the heart, four points on abdominal wall at this slice, one outside point of lateral segment on the left lobe; one bottom point of posterior segment (caudal part) on the right lobe, four points on abdominal wall at this slice. After establishing the correspondence between the landmarks, we use an interpolation transformation model of thin-plate splines [9], which is regarded as a computationally efficient method, to align the portal venous liver to the other phase livers.

### (c) *Viola-Wells mutual information based registration:*

This method [10] has been applied to image registration to deal with the images from different modalities by using gradient descent optimizer. It is intensity based and the registration transformation is determined by optimizing a similarity measure computed from the pixel intensity values of both images over the region of overlap. As no landmarks are needed, no user interaction is required and image information is not reduced to a sparse set for registration.

## 2.3 Edge detection on multi-phase 3D images

The liver tissues have a wide distribution of intensity and standard deviation in different CT images that are acquired by different modalities or parameter settings. Therefore, it is difficult to automatically determine a proper grey value as the threshold for binarization or the number of times the smoothing should be made. We propose a method by using edge

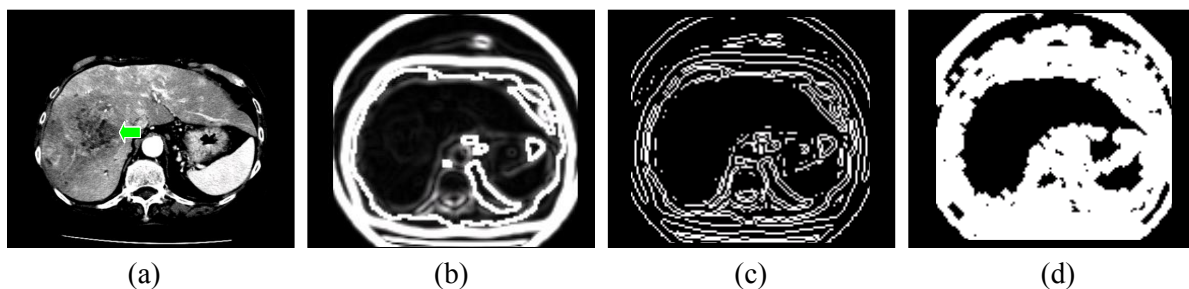


Fig. 2. Within the liver region on an original portal venous phase MDCT image (a) indicates a large HCC tumor (arrow), in which only a subtle edge leaved in magnitude map (b) derived from Sobel filter and fully disappeared in the edge map (c) by further applying LoG filter. The initial 3D liver region is turned into dark and segmented by its surface plane on the white pixels-expanded image (d).

processing to overcome these problems.

When applying the thresholding technique to separate the liver region such as those shown in Fig. 2(a), it is difficult to (1) determine a proper threshold value since the large HCC (arrow) has very different gray values and a heterogenous texture and (2) distinguish the connected organs or tissues that occasionally show relatively high or low intensities to the liver region, for example, the spleen, kidney, or the stomach. The liver can be easily recognized not only because of its large size but also its different intensity as compared to other organs that is especially obvious at the edge of a liver. Therefore, our strategy is to first focus on the edge information.

If a pixel falls on the boundary of an object in an image, then its neighborhood will be a zone of gray-level transition. Our first edge detector is the Sobel filter, which is based on convolution with an eight-directional  $3 \times 3$  derivative mask. The output of each pixel is to select one of the largest values among 8 directions after applying the Sobel masks. The benefit of this filter is that we can obtain strong edges in any direction (Fig. 2(b)) since the liver contour is closed. The use of Laplacian-of-Gaussian (LoG) operator, which has been suggested by Marr and Hildreth [11] is regarded as one of the best edge detectors. The Laplacian is applied to an image that has first been smoothed with a Gaussian smoothing filter in order to reduce its sensitivity to noise. The zero crossing detector looks for places in the Laplacian of an image where the value of the Laplacian passes through zero-points where the Laplacian changes sign. Such points often occur at edges in images. Zero crossings always lie on the closed contours, and so the output from the zero crossing detector is usually a binary image (Fig. 2(c)) with single pixel thickness lines showing the positions of the zero crossing points. By combining the Sobel and LoG filters, we can extract the subtle edges that maybe undetected when each method is used individually. After edge detection, the region of hepatic tissues as well as most of the tumor tissues are turned into black and only remains a closed contour along liver surface.

#### 2.4 Subtraction of two multi-phase images

Organs and tissues connected with liver region that have similar intensity, lesions inside the liver, or artifacts of different noises are some difficulties encountered while extracting the liver robustly in different datasets. In order to decrease the effect of these factors, we propose a new method by using the subtraction image of two phases if multi-phase images are available. Since the intensity of both the liver and the lesion regions are always lower in non-contrast phase image  $G_{pre}$  than in portal venous phase image  $G_{por}$ , subtraction value of  $G_{sub} = G_{pre} - G_{por}$  in liver region will be below zero; this will also occur in case artifacts are present. In this case,  $G_{sub}$  is regarded as 0. However, things are changed outside these areas.  $G_{sub}$  can be more than zero as the signals or noises distribute differences in the two-phase images resulting in preserving the edges. Hence, the liver and the lesion region are equal to 0 and lost edges on the subtraction image while leaving white points along the surrounding area after edge detection as shown in Fig. 2(d). Therefore, this method can effectively function in the presence of the extremely noisy images represented in white area.

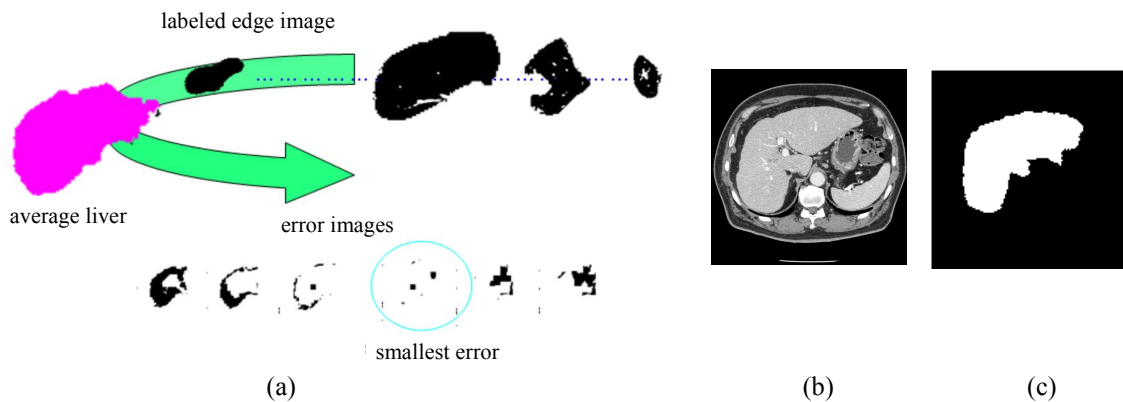


Fig. 3. After applying the procedure to detect the largest liver (a), a 2D CT slice with largest liver region (b) is selected by the average liver region (c) derived from frequency image.

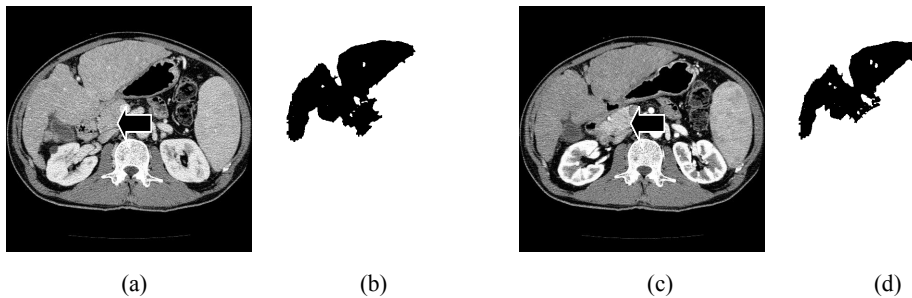


Fig. 4. An arrowed tissue region on portal venous image (a) is connected with the extracted liver region (b). This tissue has a different grey value on arterial phase image (c), and is eliminated from the final liver region (d).

## 2.5 Extraction of initial liver region and finding the slice with a largest liver

The main idea of selecting a liver region is to describe a closed surface that can hold the liver region in black as shown in Fig 2(d) as one of a 2D edge map. Thickening each point after applying LoG filter effectively reduces problems if the liver boundary is not fully closed. In our program, 4 neighbor points are expanded if a point is white in Fig. 2(c). The initial liver region, which is separated into one of the dark labels on edge map, can be picked up as the largest 3D label in the abdominal CT images except for the background. An iterate 3D morphology with labeling processing is employed for deleting the unwanted connectivity. One of the disadvantages of our previous method [3] is to manually select one of the slices with largest liver region. In order to make this procedure fully automatically, we first generate a frequency image of the liver by a range of 3D initial liver. A range of 75-mm-thick 3D liver slices are selected with 25 mm distance from the start slice and the frequency of liver points is calculated. Binarization of this frequency image derives the average shape of liver as shown in Fig. 3(c). Error images are generated from every initial liver to average liver on the right lobe, and the slice with the minimum error is selected as the slice with a largest liver region  $S_0$  in Fig. 3(c). We can observe that the shape on the right lobe of liver on the average image is very similar to the largest liver slice in Fig. 3(b).

## 2.6 Elimination of overextraction

### (a) Gray level elimination

The final liver is extracted on the portal venous phase images. The mean intensity  $G_{avr}$  and standard deviation  $SD$  of the liver within the initial liver region  $S_0$  that is derived by edge detection is calculated as a reference threshold value for binarization. Livers on CT image often appear to be homogeneous with respect to other parts. Therefore, we applied one threshold value instead of two in MRI on the original image to reconfirm the whole liver and generate the gray map, within the range of  $G_{avr} - SD$  and  $G_{avr} + SD$ . Some connectivity caused by the open edge can be easily eliminated by this processing. Starting from the  $S_0$  region, a smaller liver region is extracted by using the result of the previous slice, and this procedure stops automatically depending on the area of liver.

### (b) Neighbor shape comparing method on axial plane

Since the liver shape changes gradually slice by slice in the axial direction, connectivities with a large area can be eliminated by comparing the shape to the region of its neighboring slice. Starting from the slice with largest liver region, this procedure is applied in the direction on the upper and lower side. Some organs such as the spleen, kidney, or pancreas can be eliminated by this 2D-based processing which sometimes is impossible to realize in a 3D method.

### (c) Reference to other phase image

Some tissues or organs like the heart, pancreases, and stomach are often connected with liver and can be hardly distinguished from each other because their intensity overlaps with the liver as shown in Fig. 4(a) by an arrow. Elimination of these types of connectivity (Fig. 4(b)) is very difficult when only portal venous image is used. However, these connectivities always have different grey values as compared to the liver on arterial phase image (Fig. 4(c)), and investigation of these components facilitates elimination of ambiguous region. Within the liver region extracted from

portal venous image, all the pixels with different intensity from liver are selected as the overextracted candidates. To identify if the candidate is outside the liver region, we investigate its surrounding pixels  $S$  on portal venous image. If the mean grey value of  $S$  is near  $G_{avr}$ , then it is regarded as the vessels or tumor in liver, otherwise it is regarded as overextraction. Figure 4(d) shows an elimination example of connected tissue outside liver region.

### 2.7 Extraction of tumor candidates and integration of liver region

Since the intensity of HCC is similar to the liver region on portal venous phase images, our segmentation method does not need additional step to detect this type of lesion in the liver region. However, other hepatic tumors like hemangioma have very different intensity from that of the liver as shown in Fig. 1. Although its region is maintained by the edge detection step, it will be excluded during the re-confirmation step by binarization. In order to detect the tumor region, the mean intensity and standard deviation of the liver region that derived from edge map is calculated as a reference threshold value for binarization. The gray map is extracted on the portal venous phase images, and the tumor candidate region is identified from the difference region of the two maps. Finally, the tumor region is identified from the candidates by the features of circularity and volume. Cyst or metastasis also can be extracted by this method. The final liver region is integrated the tumor region with the liver region extracted from gray map and followed by a region growing step to extract the regions left undetected by edge detection and morphology processing.

## 3. RESULTS AND DISCUSSION

Segmentation of a 3D liver and tumor regions is completed averagely in 12 minutes running on a PC (Pentium M 1.0GHz with 512MB RAM) in our study. This is a reasonable time to be accepted by clinical uses. All the liver regions in 53 cases were successfully segmented without losing any part of hepatic lesions by a visual evaluation. In 6 cases out of the whole datasets, the average error rate on liver segmentation was within 4.3% by comparing the gold standard of liver regions drawn by radiologists with our experimental results. Eleven hepatic tumors (3 hemangioma; 4 HCC; 3 metastasis; and 1 cyst) with distinct intensity difference as compared to the liver scan on the portal venous phase MDCT images were extracted successfully and integrated into the final region. Figure 1 shows an extracted 3D liver tissue, in which a large lesion that appears as a huge hole is of the region affected by hemangioma. Other cases of normal liver or HCC tumors with only subtle intensity difference to liver are preformed with high stable results by our proposed method without losing any hepatic tissues, and detecting such HCC tumors requires the use of other methods using arterial and equilibrium phase images that appear different attenuation as in Fig. 5(b).

The time costs in employing three registration methods on a  $256 \times 256 \times 332$  3D datasets described in section 2.2 were (a) within a second, (b) 6 min, and (c) 48 min, respectively. It is obvious that the affine-based method is the fastest and there is little difference in the final liver region obtained by this method and that obtained by the other two registration methods. However, for the detection of HCC tumor, two cases with tumors smaller than 10 mm were not

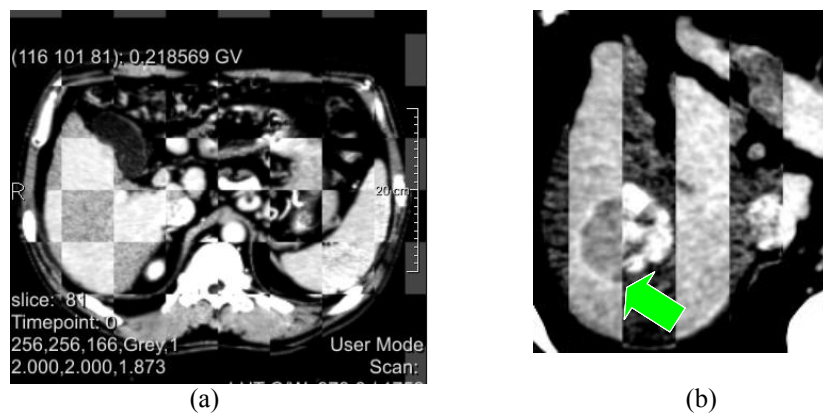


Fig. 5. (a) The registered liver region on 2D slice by different phase MDCT images is shown in different grid. (b) A HCC tumor (arrow) is successfully aligned by non rigid registration.

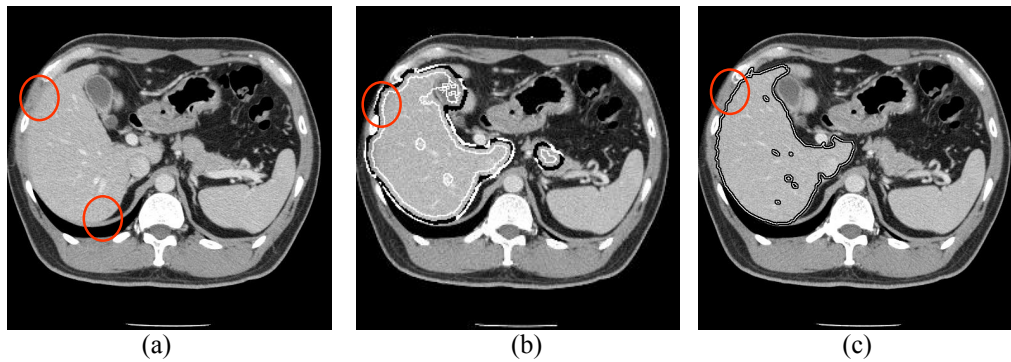


Fig. 6. The connectivities in (a) marked by circle can not be separated by the conventional thresholding technique (b) but successfully eliminated by our subtraction method (c).

detected by (a) while it was successfully extracted by (b) and (c). In case the patients changed their breathing patterns considerably during the two scanning periods, both (b) and (c) showed highly accurate registration results as shown in Figs. 5(a) and 5(b). TPS can realize the non-rigid registration in a reasonable time but requires the manual placement of landmarks, while in the mutual information registration no landmark and user interaction are required; however, it is an extremely time consuming method. Therefore, in our LiverCAD system, affine-based registration is sufficient for liver segmentation due to the large size of the liver and the subsequent region growing procedure. Non-rigid registration is required when extending this method to multi-organ extraction when the target organs are smaller in size. TPS appears to be more practical in clinical use but more sophisticated and robust algorithms have to be developed to automatically extract the landmarks in the next step.

Our program can be used with a single phase or multi-phase mode, which implies that the flexibility and utility of our LiverCAD system for the clinical uses as the number and time series of scanning varies in different hospitals. The multi-phase mode allows subtraction process and thus improves the accuracy of segmentation than using only one-phase image. Furthermore, this method will be modified to enable the use on MRI.

On the subtraction image of two phases there is no edge inside the subtracted liver or other enhanced organ regions; thus, this method also has been extended successfully to the multi-organs extraction. The main method of segmentation of the organs is based on edge processing, and the thresholding technique is used only in the elimination of connectivities. Since no mean intensity or standard deviation is required to estimate the initial extraction, our proposed method can be used effectively on different datasets even if the images are very noisy or contain heterogeneous tissues. In this experiment, three different datasets from various countries are involved in the testing materials and all the livers and tumors are extracted successfully by our method.

Out of all the results we did not encounter any problem of overextraction along the abdominal wall that frequently occurred in the conventional method (Fig. 6(a)). This is due to effect of subtraction processing. The positions where the muscles were connected to liver were different in different phase image, and such overextraction could be easily eliminated by the subtraction method as shown in Fig. 6(b).

#### 4. CONCLUSIONS

We proposed an automatic method for the extraction of the liver region with tumors tissues on multi-slice MDCT. It has been proven that our non-intensity based edge-detection and subtraction method can function effectively on the datasets from different modalities with different image quantities despite the presence of hepatic lesions within the liver. The result demonstrates that our program is promising and effective in the segmentation of the liver region, and it is expected to be useful in the clinical examination of an in vivo hepatic radiographic image.



## 5. ACKNOWLEDGMENTS

This research was supported in part by the Ministry of Health, Labour, and Welfare under a Grant-In-Aid for Cancer Research and in part by the Ministry of Education, Culture, Sports, Science and Technology under a Grant-In-Aid for Scientific Research, Japanese Government.

## REFERENCES

1. H. El-Serag and A. Mason, "Rising incidence of hepatocellular carcinoma in the United States," *N. Engl. J. Med.*, Vol. 340(10), pp. 745–50, 1999.
2. X. Zhang, M. Kanematsu, H. Fujita, T. Hara and H. Hoshi, "Computerized classification of liver disease in MRI using artificial neural network", *Proc. SPIE*, Vol. 4322, pp. 1735–1742, 2001.
3. X. Zhang, W. Li, H. Fujita, M. Kanematsu, T. Hara, X. Zhou, H. Kondo and H. Hoshi, "Automatic segmentation of hepatic tissue and 3D volume analysis of cirrhosis in multi-detector row CT scans and MR imaging," *IEICE*, Vol.E87-D, No. 8, pp. 2138–2147, 2004.
4. T. Hitosugi, A. Shimizu, M. Tamura, and H. Kobatake, "Development of a liver extraction method using a level set method and its performance evaluation", *Journal of Computer Aided Diagnosis of Medical Images*, Vol.7, No.4, 2003 (in Japanese).
5. L. Gao, D. Heath, B. Kuszyk, and E. Fishman, "Automatic liver segmentation technique for three-dimensional visualization of CT data", *Radiology*, Vol. 201, No. 2, pp. 359–364, 1996.
6. J. Masumoto, M. Hori, and Y. Sato, "Automated liver segmentation using multislice CT images," *IEICE*, vol. J84-D-II, no.9, pp. 2150–2161, 2001 (in Japanese).
7. K.Bae, M. Giger, and C. Chen, "Automatic segmentation of liver structure in CT images," *Med. Phys.* vol. 20, no.1, pp.71–78, 1993.
8. H. Park, P.H. Bland, and C.R. Meyer, "Construction of an abdominal probabilistic atlas and its application in segmentation," *IEEE Trans. on Med. Imag.*, Vol. 22, no.4, pp.483–492, 2003.
9. F. L. Bookstein, "Principal warps: Thin-plate splines and the decomposition of deformations," *IEEE Transactions on Pattern Analysis and Machine Intelligence*, Vol. 11, No. 6, pp. 567–585, Jun. 1989.
10. W. Wells, P.I. Viola, H. Atsumi, S. Nakajima and R. Kikinis, "Multi-modal volume registration by maximization of mutual information", *Medical Image Analysis*, Vol. 1(1), 35–51, 1996.
11. D. Marr and E. Hildreth, "Theory of edge detection," *Proc. Royal Society of London*, B207, pp. 187–217, 1980.